Real-Time Observation of Multiexcitonic States and Ultrafast Singlet Fission Using Coherent 2D Electronic Spectroscopy

Artem A. Bakulin*[1,2], Sarah E. Morgan[2], Tom B. Kehoe[2], Mark W.B Wilson[2], Alex Chin*[2], Donatas Zigmantas[4], Dassia Egorova*[3], Akshay Rao*[2]

[1]*FOM Institute AMOLF, 1098 XG Amsterdam, The Netherlands*
[2]*Cavendish Laboratory, University of Cambridge, JJ Thomson Avenue, Cambridge CB30HE, UK*
[3]*Institut für Physikalische Chemie, Christian-Albrechts-Universität, Olshausenstr. 40, D-24098 Kiel, Germany*
[4]*Department of Chemical Physics, Lund University, P.O. Box 124, 22100 Lund, Sweden*

**Corresponding authors*
aab58@cam.ac.uk, ac307@cam.ac.uk, degorova@gmail.com, ar525@cam.ac.uk

Abstract:

Singlet fission is the spin-allowed conversion of a spin-singlet exciton into a pair of spin-triplet excitons residing on neighbouring molecules. To rationalise this phenomenon, a multiexcitonic spin-zero triplet-pair state has been hypothesised as an intermediate in singlet fission. However the nature of the intermediate states and the underlying mechanism of ultrafast fission have not been elucidated experimentally. Here, we study a series of pentacene derivatives using ultrafast 2D electronic spectroscopy and unravel the origin of the states involved in fission. Most importantly, our data reveal the existence of a vibronic manifold of multiexcitonic triple-pair states, which strongly mix with the singlet excitons. This distribution of states with mixed singlet/triplet-multiexciton character drives sub-100-fs fission with unity efficiency. Our results provide a new framework for understanding singlet fission and show how the formation of vibronic manifolds with a high density of states facilitates fast and efficient electronic processes in molecular systems.

Main text:

Singlet fission (SF) is an exciton multiplication process in organic semiconductors that allows one photogenerated spin-singlet excited state to be converted to two spin-triplet excitons.[1] The two generated spin-triplet excitons are initially correlated to form an overall spin-singlet state, making SF a spin allowed process in contrast to intersystem crossing that involves a spin flip. For systems where the energy of the lowest lying singlet exciton (*S*) is close to double energy of the triplet state (*T*), such as pentacene and its derivatives, SF can occur on a sub-100 fs timescale with every singlet being converted to two triplets.[2]

SF has attracted great attention lately as it enables photovoltaic devices to overcome thermalisation losses by generating two electron-hole pairs per high-energy photon absorbed, potentially allowing single-junction devices that could beat the Shockley-Queisser limit on power conversion efficiency[3]. The first steps towards this goal have been taken with the demonstration of organic solar cells based on pentacene, that show external quantum efficiencies above 129%, the highest for any solar technology to date.[4, 5]

Despite advances in the experimental characterization of SF in several molecular systems [6-13] as well as extensive theoretical work,[1, 14-22] the fundamental mechanism of ultrafast SF remains unclear. In the kinetic model proposed by Merrifield and co-workers[23] the process can be represented as

$$S \rightarrow TT \rightarrow T+T$$

Where: *S* is the lowest singlet excited singlet state, *T* is the molecular triplet state and *T*+*T* is a pair of fully independent *T* states. *TT* corresponds to a doubly excited pair of spin-correlated triplets, forming an overall spin singlet. The *TT* state, often referred to as the multiexciton state, is considered a dark state that cannot be optically populated from the ground state (*g*), but serves as an intermediate to the formation of free independent triplets (*T*+*T*).

Current theoretical models for SF focus on characterising the electronic structure of the *S* and *TT* states, and the interplay between them.[1, 20, 21] While it is clear that the coupling between *S* and the *TT* state controls the dynamics of the fission, the nature of this coupling is hotly debated. The proposed mechanisms include the `direct' two-body coulomb coupling [24] and the presence of an intermediate double triplet state which is degenerate with the singlet exciton [25, 26]. Recent studies propose that the `indirect' coupling, mediated by the mixing of the singlet and triplet excitations with charge-transfer excitons dominates the interaction,

leading to reported coupling values in the range 0.02-0.11 eV (200-900cm$^{-1)}$.[14, 18, 24] There is some debate over the energies of the charge-transfer states and whether they participate as nactual intermediates in the SF process, or as virtual states that mediate effective coupling of *S* and *TT* via a type of 'super-exchange'. [15] Some recent theoretical work has also begun to evaluate the influence of molecular motion in modulating the coupling between *S* and *TT* .[18, 19 27] In contrast to the wealth of theoretical studies, there are very few [25, 26 28 29]experimental studies that provide an insight into the nature of the *TT* state, the couplings between the singlet and *TT* manifolds, or how these couplings are effected by molecular motions and energies of vibrational states. It is thus clear that, to judge the reliability of theoretical methods and to build up a comprehensive mechanistic picture of SF, new types of experiments accessing both the electronic and vibrational phenomena are needed.

Here we use ultrafast 2D electronic photon echo spectroscopy (2DES) to access both the electronic and coupled vibrational dynamics of SF in a series of pentacene derivatives. The unique transition-pathway selectivity and high time resolution (<15 fs) of this technique allow us to observe a number of previously experimentally inaccessible intermediates in the SF process. Combined with a theoretical model, which reproduces the 2DES data, we show that vibrational modes serve to couple the 'bright' *S* and 'dark' *TT* excitons, generating a vibronic manifold of mixed singlet/triplet-multiexciton states that mediate the ultrafast SF process.

2DES spectroscopy is four-wave mixing technique, in which three pulses interact with the system to produce a fourth 'signal' field, interferometrically detected in a phase-matched direction.[30] The 2DES approach used here combines sub 15-fs time resolution with a high selectivity in excitation (ω_{ex}) and probe (ω_{pr}) light frequencies, in contrast to pump-probe spectroscopy that does not allow resolution on the excitation frequency. This allows for selective discrimination of the responses related to different excitation pathways, addressing the effects of electronic and vibrational coherences and, therefore, provides more extensive information about the underlying photophysics.[31-39]

We study pentacene and its derivatives 6,13-di(2′-thienyl)pentacene (DTP) and 6,13-bis(triisopropyl-silylethynyl) pentacene (TIPS) as model systems for ultrafast fission, all of which undergo SF on the ~100-fs timescale.[11] The ultrafast nature of the process is important as it allows SF to outcompete other single exciton relaxation channels such as radiative decay, excimer formation, intersystem crossing and charge transfer. Figure 1a shows the molecular structure and energy levels of the materials. These molecules share the

pentacene aromatic core but have different side groups, which cause them to pack differently in the solid state leading to the different intermolecular couplings.[11] Material absorption spectra, shown in Figure 1b, indicate substantial differences in the energy of singlet states. Based on the absorption data, the lowest singlet state lies at 1.75eV for TIPS, 1.83 eV for pentacene and 1.86 eV for DTP. The energy of the triplet state is however not expected to differ for these systems, since the triplet is localised on the aromatic core of a single pentacene molecule.[40] This energy has previously been measured to be 0.86 eV and the energies of the double-triplet *TT* state for all the systems are therefore expected to lie around 1.72 eV.[24] Figure 1b also shows the spectrum of the 15-fs laser pulse used in the experiments. The spectrum is broad enough to cover the regions of singlet absorption for all the pentacene derivatives and the spectral region corresponding to the predicted energy of the *TT* state.

Figure 2 presents three time frames showing the evolution of the real-part of the 2DES spectra for a polycrystalline pentacene film (for a movie evolution of 2D spectra with time see SI). The sample was tilted by ~50 degrees with respect to the incident beam to enhance the response of the triplet component, as has been previously discussed.[41] The 2D spectra are dominated by a large positive peak on the diagonal at 1.83 eV, which corresponds to ground-state bleach (GSB) of the main singlet transition *g*-*S* and at short times (<90 fs) also includes a contribution from stimulated emission (SE) from the singlet exciton.[42] At 30 fs, a photoinduced absorption (PIA) feature, seen as negative peak at 1.85 eV probe energy, is present. We assign this feature to the excited state absorption (ESA) of singlet excitons S-S_n in agreement with previous pump-probe measurements.[41] At longer waiting times, this ESA is lost as singlets undergo fission and two new PIA features at 1.70 eV and 1.88 eV probe energy appears. These new peaks are assigned to the transition from the lowest triplet state *T* to the higher lying T_2 and T_3 states respectively.[42] Importantly, no feature is observed at excitation energy of 1.72 eV where the *TT* state is predicted to be. The signal is close to zero at all evolution delay times, which indicates that negligible response cannot be a result of interference between singlet and triplet contribution. This confirms that the *TT* state has negligible (much smaller than *S*) transition dipole. The spectra for TIPS and DTP are very similar with the singlet peak shifted in agreement with the absorption spectra (see SI).

To confirm the identification of different contributions to the signal and to determine the interconversion rates between different electronic states we de-convolute the 3D (ω_{ex}, ω_{pr}, $T_{evolution}$) data matrix into 2D decay-associated spectra. For pentacene, the analysis reveals

three components with the characteristic time scales of 14 fs, 83 fs, and >>1 ps (see SI for spectra). The fastest timescale corresponds to pulse overlap situation and is assigned to the coherent artefact. The spectral configuration of the long-lived component match the spectra of triplet previously observed in pump-probe measurements.[42] Finally, the spectra and decay time of the 83 fs component reflect the singlet to triplet conversion (*S* and *T* response difference) and are in excellent agreement with previous assignments of the singlet exciton from pump-probe studies; the observed 83-fs time constant thus represents SF rate. [41] Kinetics for TIPS and DTP are very similar with SF rates of 100 fs and 130 fs (see SI).

Figure 3a shows the representative kinetics of the real part of the 2D spectra of pentacene (Figure 2), corresponding to (i) *g*-*S* GSB/SE, (ii) *T*-T_2 ESA, and (iii) at $\omega_{ex}=\omega_{pr}$=1.72 eV which is the expected position of *g*-*TT* GSB. The red curve represents a global fit to the data using the three components described above. The model reproduces the data well, except for the oscillations which can be clearly seen in all three traces. The oscillations are found to be present even at (1.72 eV, 1.72 eV). At this position the average population is negligible and the signal beats around zero. The frequency of the oscillations does not match an energy difference between electronic states, indicating that these oscillations do not arise from electronic coherence. Alternately, the beatings could be caused by short-pulse induced superposition of vibonic states in the electronic ground or excited states manifolds. Such an effect, known as vibrational coherence, contains information about the evolution of vibrational wave-packets and the couplings between the vibrational and electronic dynamics.

The beatings seen in Figure 3a are long-lived, lasting over 1500 fs, which suggests that they more likely to originate from the vibrational coherence,[32, 33, 43] as electronic dephasing times in molecular systems are typically less than 100 fs at room temperature.[44] To explore this further, we Fourier transform (FT), along the $T_{evolution}$ axis, the residual obtained by subtracting the global fit (red curves) from the experimental data (blue curve). The FT spectra obtained for pentacene, TIPS and DTP (Figure 3b, blue curves) show a clear structure with up to ten peaks having a bandwidth of <20 cm^{-1}. The red curves in Figure 3b present steady state resonant Raman measurements for each material. All the peaks in the FT spectra are found to correlate well with the modes observed in the Raman measurements. Additionally, the shape and amplitude of the FT spectra do not change dramatically in time for any of the three materials. Crucially, there are no features in the FT spectra that could correspond to the energy difference between *S* and *TT*, 0.11 eV = 890 cm^{-1}. Hence, there is no

evidence for long-lasting electronic coherence between *S* and *TT* mediating the singlet fission process. Thus, the comparison between the FT of the oscillatory part of 2DES response and the Raman spectra gives a strong indication of the vibronic origin of the beatings observed.

The high quality of the experimental data allows us further analyse the vibrational beatings and achieve additional insight into excited- and ground-state vibronic dynamics. For this, we chose the most intense vibrational modes (shown in fig. 3b) and, for each of them, plot a 2D map of the amplitude of the oscillatory component of the response, as a function of excitation and probe frequency (ω_{ex} and ω_{pr}). This yields the 2D 'beating-maps'[32] that are shown in Figure 4 for 265 cm^{-1}, 605 cm^{-1}, 1170 cm^{-1}, 1360 cm^{-1} (0.032eV, 0.075eV, 0.145eV, 0.169eV) vibrational modes observed in the FT and resonance Raman spectra of pentacene film (Figure 3b). Similar maps for TIPS and DTP are presented in the SI.

For all the 2D beating maps presented in Figure 4 an intense peak is found in the 'diagonal' region of $\omega_{ex}=\omega_{pr}=\omega_S= 1.83\ eV$, which corresponds to the lowest singlet exciton level. In addition, multiple off-diagonal peaks are observed at $\omega_{ex} = 1.83\ eV$. As shown by the arrows in Figure 4, these peaks are displaced from the diagonal peak along the probe axis roughly by the energy corresponding to the vibrational mode considered in the beating map.[32, 33] For example, in the 605 cm^{-1} (Figure 4b) beating map peaks can be seen at probe frequency $\omega_{pr}=\omega_S$ - 605 cm^{-1} while the 1170 cm^{-1} beating map shows a peak at $\omega_{pr}=\omega_S$ - 1170 cm^{-1} (figure 4c). These and additional peaks that occur below and to the right of the diagonal (dashed line in figures) are caused by the coupling of vibrational modes to an electronic transition. The exact shape of the beating pattern is complex and different for the rephasing and non-rephasing parts of 2DES response. However, our observation of beating peaks for $\omega_{ex}>=\omega_S$ (1.83 eV) can be described within the theoretical framework considering vibrations coupled to a single electronic state.[32, 33, 43]

The above described peak pattern for $\omega_{ex}>=\omega_S$ (1.83 eV) is associated with the GSB signal and, as such, predominantly reflects the dynamics of the ground-state vibrational coherence.[33] However, the beating maps in figure 4 clearly contain more peaks, especially for the high-frequency 1170 cm^{-1} and 1360 cm^{-1} oscillatory modes. Most of these additional peaks are located at the excitation frequency $\omega_{ex}\sim$ 1.72 eV which is below the singlet transition and therefore cannot be described by GSB signals and ground-state coherences from the singlet vibrational manifold. However, this energy coincides with the expected position of *TT* state, suggesting that the additional peaks could be associated with transitions

from ground to multiexction state. Such a transition would have a transition dipole much smaller than that of singlet excitation, making it indistinguishable in the linear absorption spectrum, where it would be obscured in the tail of the *S* absorption feature. However, as the intensities of the peaks in beating maps are determined by four different interactions with the field, [43] and even if one of the transition dipoles is very low (i.e a 'dark' transition), the product of interactions and the intensity of the beating peak can be significant. In essence, the vibrational dynamics presented in beating maps may reveal transitions normally hidden in linear absorption or smeared out in the measurements addressing population dynamics. [32, 33, 35]

To unravel the rich data provided by the beating maps, on the coupling between electronic states and vibrational modes, we construct a model that explains, qualitatively and quantitatively, all the features observed in the beating maps, and reproduces the experimental 2DES dataset. Here we will qualitatively describe the model while a detailed quantitative picture is presented in the Supplementary Information. First of all, the involvement of *TT* state in the formation of beating patterns implies that coherent superpositions of *TT* and some other states, displaced by certain vibrational frequencies, are being excited. These other states can be assigned to the vibronic multiexciton manifold (*TT')* (Figure 1). Importantly, some states within this manifold have energy close to that of the singlet; for pentacene these states are TT'_{1170} and TT'_{1360}, which lie at *TT*+1170 cm^{-1} and *TT*+1360 cm^{1} respectively (Figure 1a). This allows for partial mixing of the singlet and multiexcitons *TT'* even by means of modest electronic coupling (248 cm^{-1}). Such mixing may not substantially alter TT'_{1170} and TT'_{1360} energies, but it may make those states 'bright' and observable in the beating spectra.

Figure 5a,b explains the different contributions to the 1170 cm^{-1} and 1360 cm^{-1} rephasing/non-rephasing beating maps using the assumptions discussed above. Optical transitions occur between four electronic states: the ground state g, the lowest singlet *S*, multiexciton *TT*, and TT_3 - an excited multiexciton state formed via the $T\text{-}T_3$ transition for one of the triplets, which is known to lie at 2.38 eV for pentacene. We also consider the vibrationally hot ground *g'* and mulitexciton *TT'* states. Figure 5b depicts the four-wave-mixing pathways where a superposition of states is created after the first two interactions and mark the corresponding peak positions in the beating maps. We excluded *g-TT* GSB/SE contributions as it requires two interactions with the almost dark *TT* state, and *S-g* SE contribution due to the short lifetime of *S* state. Finally, we consider the initial thermal population of vibrationaly excited ground states *g'* negligible.

Within the above framework we can describe all the peaks in Figure 5a. Peaks *1-2* are due to the ground-state vibrational coherence and GSB of *S* state. Peaks *3-4* correspond to creating a coherent superposition in the excited state, between *TT* and *TT'*, which is observed through the transition to a higher-lying TT_3 state. As seen from the diagrams, at least three out of four interactions involve bright states; this makes the total amplitude of the beating peaks significant. Thus, the proposed qualitative model accurately explains the peaks in the beating maps, providing strong evidence that our observations reveal a vibronic manifold of multiexcitonic states.

This interpretation is supported by the appearance of additional peaks *3,4* only for high-frequency vibrations. As shown in Figure 1a the *TT*, TT'_{265} *or* TT'_{605} states are energetically much further from *S* then TT'_{1170} and TT'_{1360} which prohibit them from 'borrowing' the oscillator strength and keeps them dark. This leads to the disappearance of peaks *3-4* from 265 cm^{-1} and 605 cm^{-1} beating patterns as observed in figure 4. Consistent with the above interpretation, figure 5c shows that in case of TIPS (but not DTP) the *3-4* beating features appear for lower 265 cm^{-1} vibrational mode, as the smaller gap between *S* and *TT* brings the TT'_{265} mode almost in resonance with the TIPS singlet exciton (fig. 1a).

To confirm the assignment of the observed coherences to the singlet-multiexciton mixed excited states and support the proposed interpretation, we have undertaken a set of complementary experiments and analysis, developed to identify the nature of coherent states. While detailed results and discussions can be found in SI, here we summarise the main findings. A phase analysis[45] of the beatings confirms the excited-state nature of peaks 3 and 4 and the ground-state origin of peaks 1 and 2. Polarisation-selective measurements[46] reveal that the beating features 3 and 4 for high-frequency vibrations are associated with mixed electronic states, e.g. singlet-multiexciton mixtures. Finally, complimentary 2D measurements in a different spectral range, 2-2.4eV, support the assignment of ESA features and confirm the existence of long-lived excited state coherence, coming from the mixed vibronic states.

To quantitatively extend the analysis, we construct a vibronic state model of the observed SF dynamics. This model can quantitatively reproduce the 2D photon-echo data, including the beating map patterns. Importantly, the same set of parameters capture the vibronic level structure, the spectroscopic observables and the ultrafast dynamics of the SF process. The model consists of three Raman active modes (265 cm^{-1}, 1170 cm^{-1}, and 1360 cm^{-1} with Huang-Rhys factors 0.7, 0.6 and 0.75 respectively) and two coupled electronic states.

One of the electronic states is assumed to be optically bright and represents the *S* singlet electronic excitation coupled to the Raman modes. The second electronic state is chosen as optically dark and represents the multiexciton state. The electronic coupling between singlet and multiexciton manifolds employed in the model (248cm^{-1} = 0.031eV) is small compared to the energy difference between the S and TT states (~900cm^{-1} = 0.11eV). To adequately model the spectroscopic response, the electronic ground state as well as a higher-lying electronic state (ESA occurs to this state) with their vibrational manifolds are explicitly considered as well, although they do not have any impact on the excited-state dynamics relevant for the fission process. We also introduce a weak linear coupling to a harmonic bath, as described within the multilevel Redfield approach.[47] Full details of the model can be found in the SI.

Using the above parameters we modelled the structure of the vibronic manifold, 2DES beating maps, and the population kinetics for the excited states during SF in pentacene. Partial mixing of *S* and *TT* vibronic manifolds leads to the formation of a dense manifold of 16 new eigenstates (figure 6a). The lowest four possess mostly (95%) multiexciton contribution, the fifth lowest state is dominantly singlet, and higher-lying states have a more mixed character. The dipole moments of these states vary significantly, however even the lowest state (close to diabatic *TT*) is not completely dark. The calculated oscillator strength agree well with the absorption spectrum of pentacene (figure 6b), indicating that the 'dominantly-multiexcitonic' absorption feature is likely to be present, but hidden under the broad and intense 'dominantly-singlet' features. The modelled beating maps are also in a good agreement with the experimental data (compare figures 6c and 5a), showing that the model accurately captures the underlying photophysical processes. The dynamics produced by the model (fig. 6d) show that the total population of optically bright states decays on a 83-fs timescale, consistent with the singlet-triplet conversion rate reported here and in previous pump-probe studies. [41]

Interestingly, due to the mixed character of the initially photoexcited states, the total multiexcitonic (dark) population 12 fs (pulse duration) after excitation is significant, which is in good agreement with the near instantaneous rise of a triplet feature observed by Zhu and co-workers using time-resolved photoemission measurements.[25, 48] However, as described above, we attribute this signal to the mixed electronic characters of the vibronic eigenstates, rather than to strong electronic coupling between the singlet and a single degenerate multiexciton state as proposed by Zhu et al. Based on our data, we propose that the cooling

process observed by Zhu et al. on a 200-fs timescale corresponds to vibrational cooling of eigenstates of predominantly triplet character (see SI).

The crucial role of the vibronic-manifold of states for fast and efficient SF reveals the general importance of nuclear degrees of freedom for the optoelectronic properties of organic materials. In contrast to the classical inorganic semiconductors, molecular systems suffer from weak intermolecular interactions and high disorder, which prevents the formation of delocalised all-electronic band states. However, coupling of the electronic system to multiple intramolecular vibrational modes creates vibronic manifolds with a high density of states. These dense manifolds can facilitate efficient coupling between different molecules (or intramolecular states) even when only weak interactions are present. Indeed, coherent vibronic phenomena has recently been proposed to be crucial to electronic processes in organic photovoltaics[49] and natural photosynthetic systems.[50]

In conclusion, using 2DES, we observed a manifold of multiexcitonic states mediating ultrafast SF in pentacene and its derivatives. Our observations and modelling indicate that overlap and mixing of the vibronic manifolds of singlet exciton and multiexcitonic state play a key role in ultrafast dynamics of SF. In particular, the presence of these mixed states means that strong electronic couplings, exceeding the energy difference between the singlet and the multiexcitonic state, are not required to allow for sub 100 fs conversion between singlet and triplet states. Our data not only provide firm experimental evidence of the importance of vibronic coupling and mixed intermediate states in the fission process, but may also serve as the basis for future theoretical models of the photophysics of a broad class of organic chromophores that could allow such mixed states.

Acknowledgements:

We thank Thomas Jansen and Maxim Pschenichnikov for useful discussions and David Palecek for the help with ~580 nm 2D experiments. This work was supported by Laserlab-Europe (Project:LLC001945). A.A.B. is currently a Royal Society University Research Fellow, he also acknowledges a Veni grant from the Netherlands Organization for Scientific Research (NWO). A.R and A.C thank the Winton Programme for the Physics of Sustainability for support.

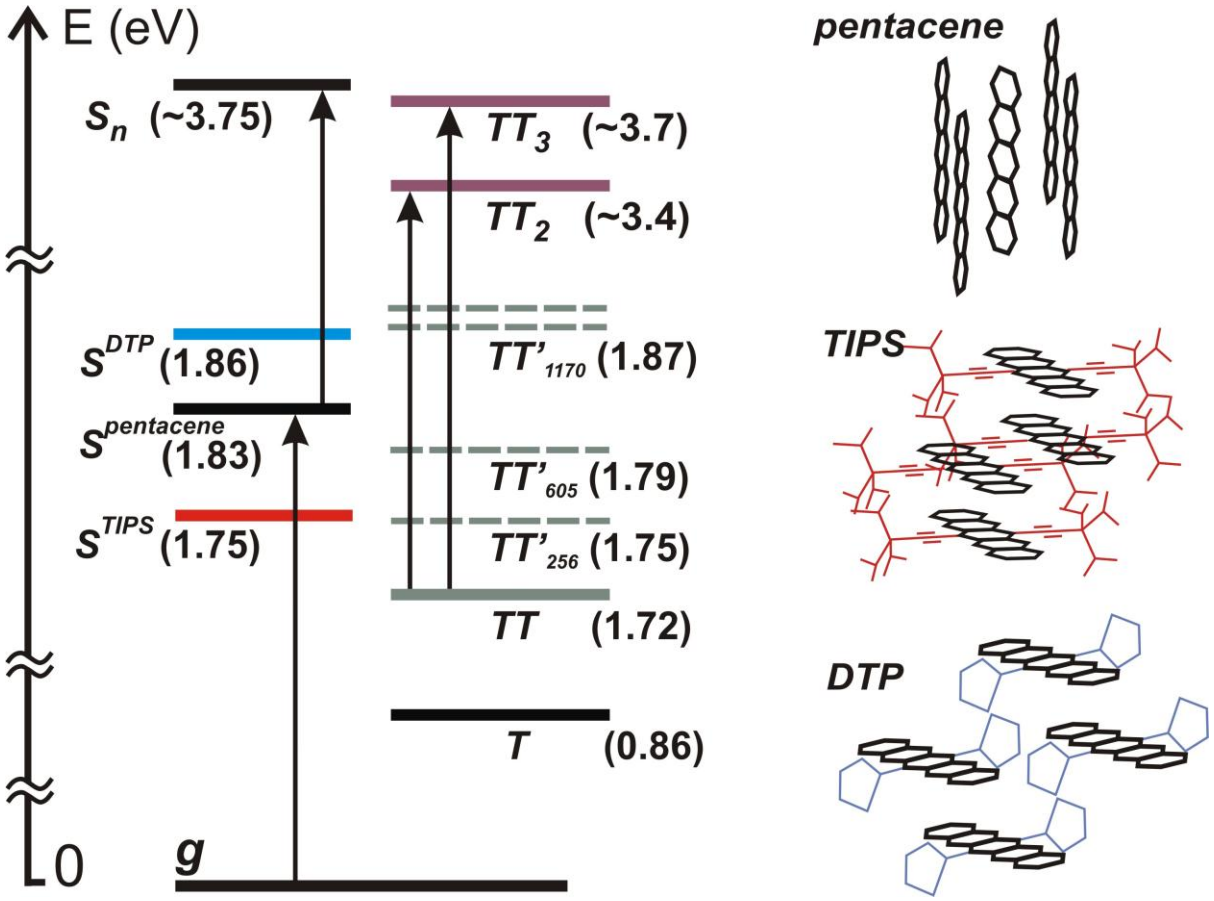

Figure 1a. *The free-energy diagram depicting electronic and vibronic (marked with ‘) states addressed in the 2DES experiments and the molecular-crystal structure of the systems under study. The numbers show approximate energies of the states in eV.*

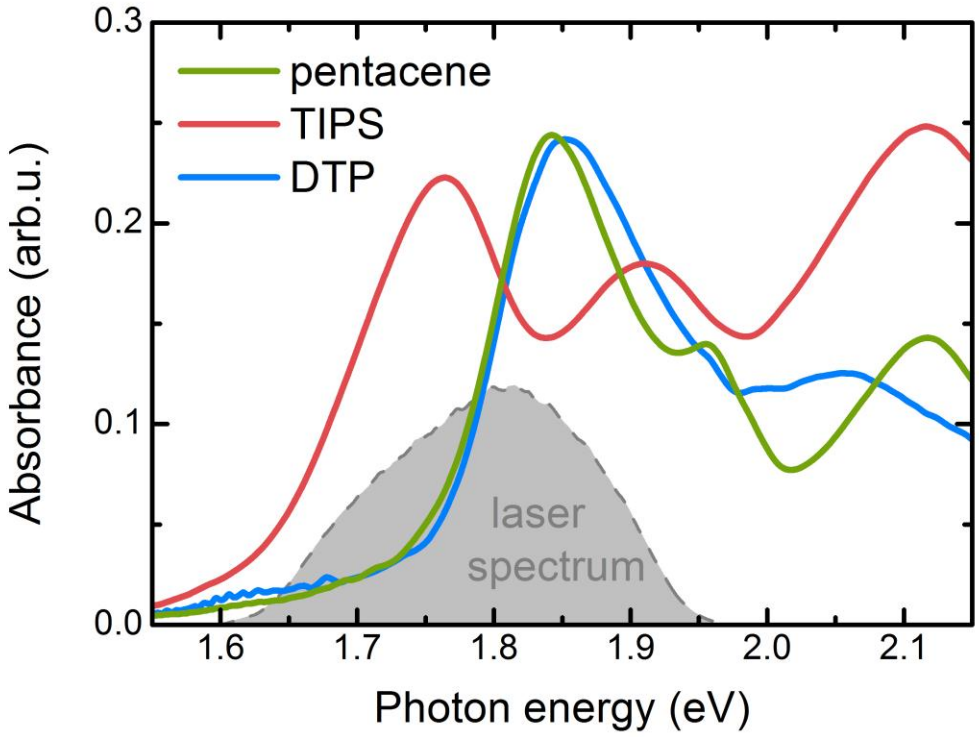

Figure 1b. *The absorption spectra of the films under study. The grey contour presents the laser spectrum used in 2DES experiments.*

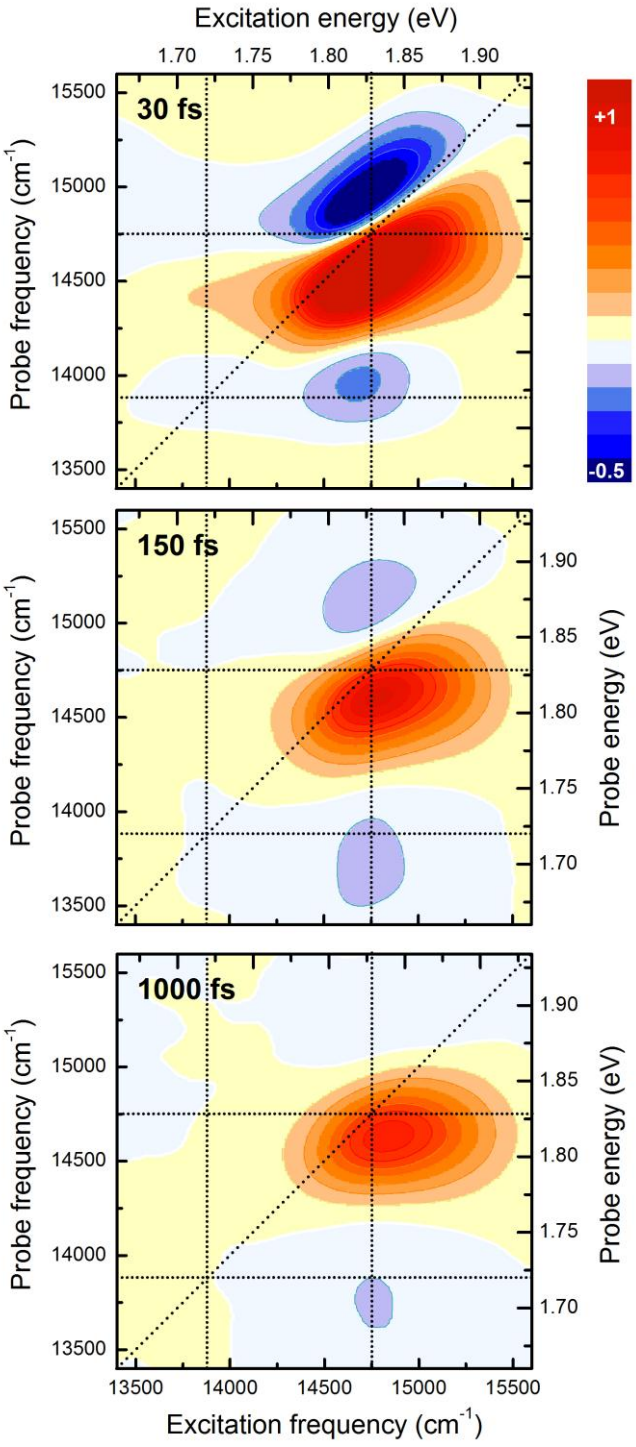

Figure 2. *2DEPE real-part spectra of pentacene molecular crystal at different evolution times.*

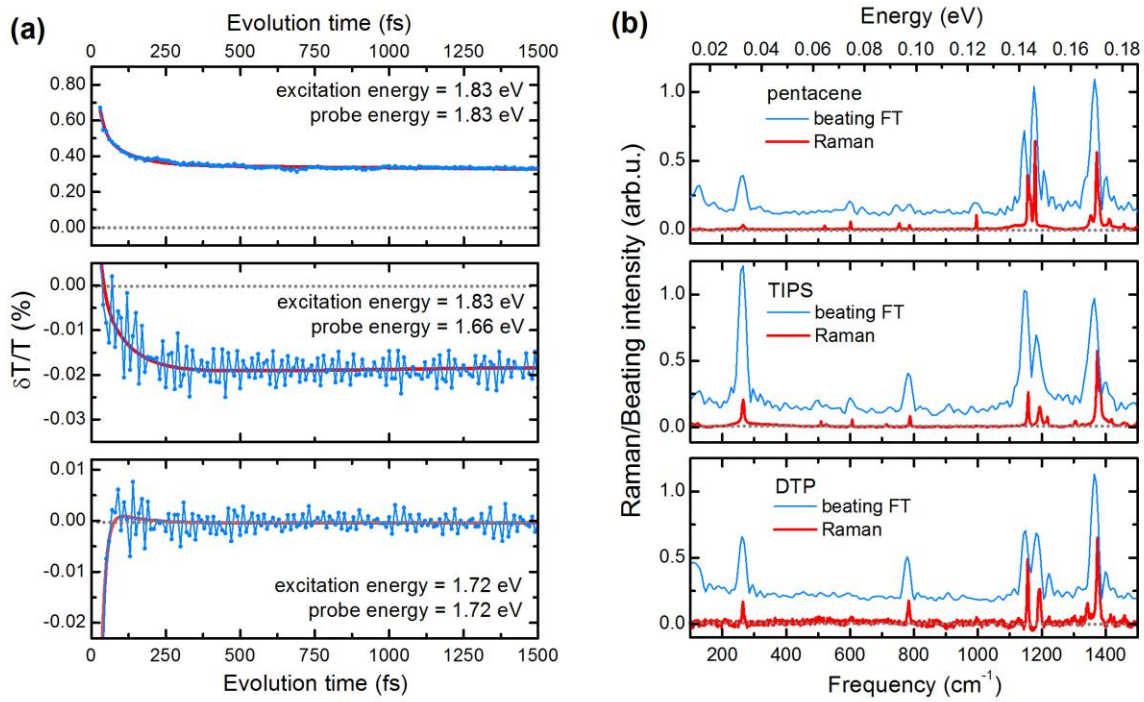

Figure 3. *(a) Blue curve shows evolution-time transients corresponding to the different locations in the 2D spectrum of pentacene. Red curve is the description of the population dynamics by the 3-component decay-associated spectra. (b) Spectrum of evolution-time oscillations observed in 2DES data integrated over complete 2D spectrum compared to the resonance Raman spectrum of films of pentacene and its derivatives.*

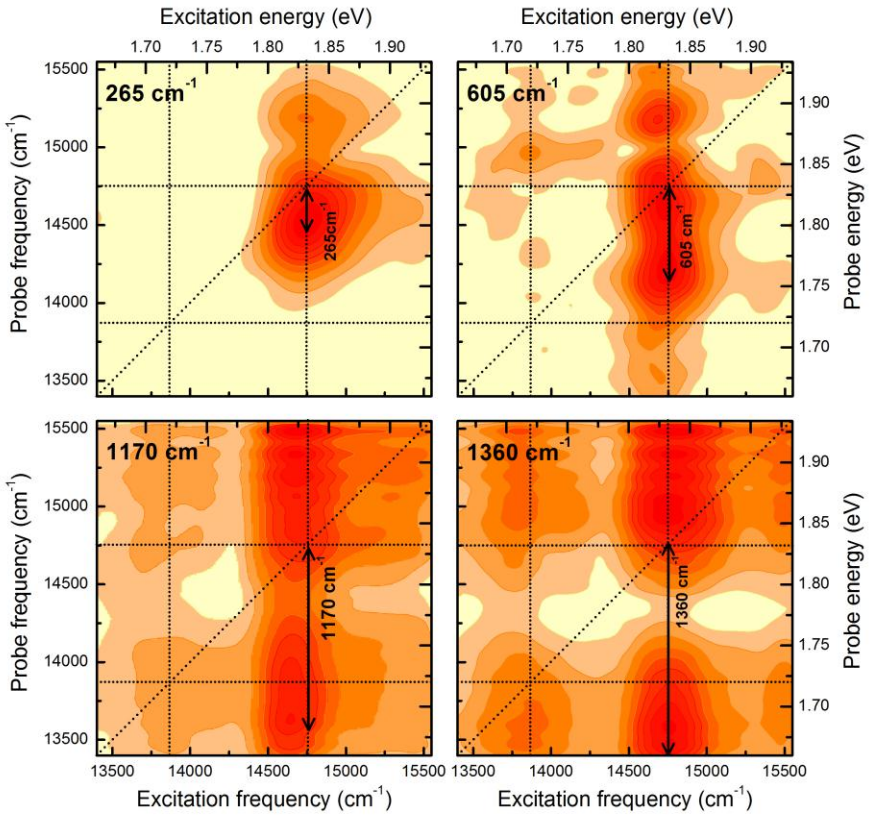

Figure 4. *The 2D maps of beating in 2DES spectra corresponding to the strongest oscillatory features observed in figure 3b.*

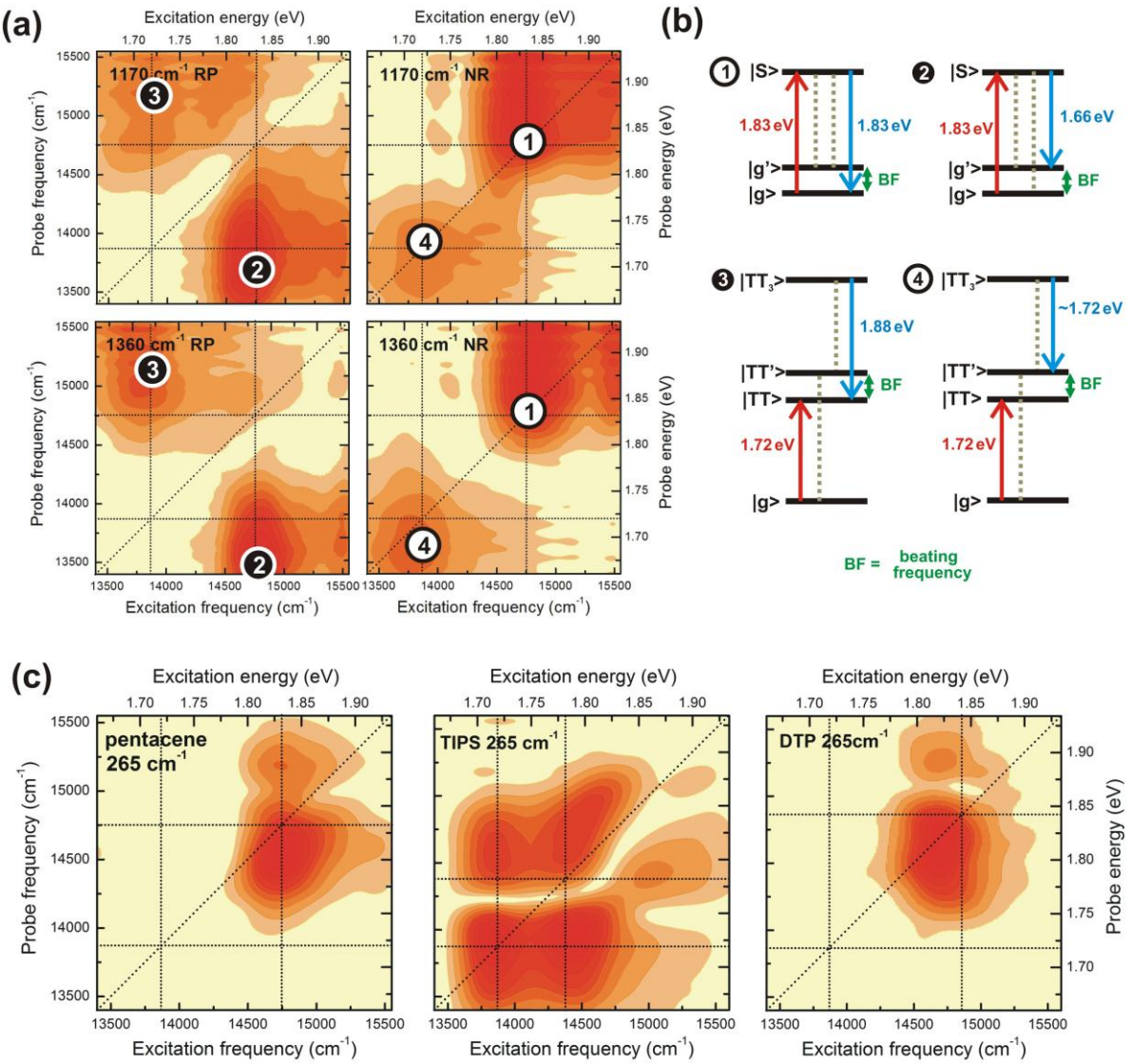

Figure 5. *(a) The rephasing and non-rephasing part of 2D beating maps corresponding to observed high frequency vibrational modes of pentacene. Diagrams present the relevant system-field interactions and the numbers mark the corresponding positions of the beating peaks. Rephasing features are marked with black and non-rephasing with white circles. (b) The 2D maps of beating maps corresponding to the 265 cm^{-1} oscillatory features observed in pentacene and its DTP and TIPS derivatives.*

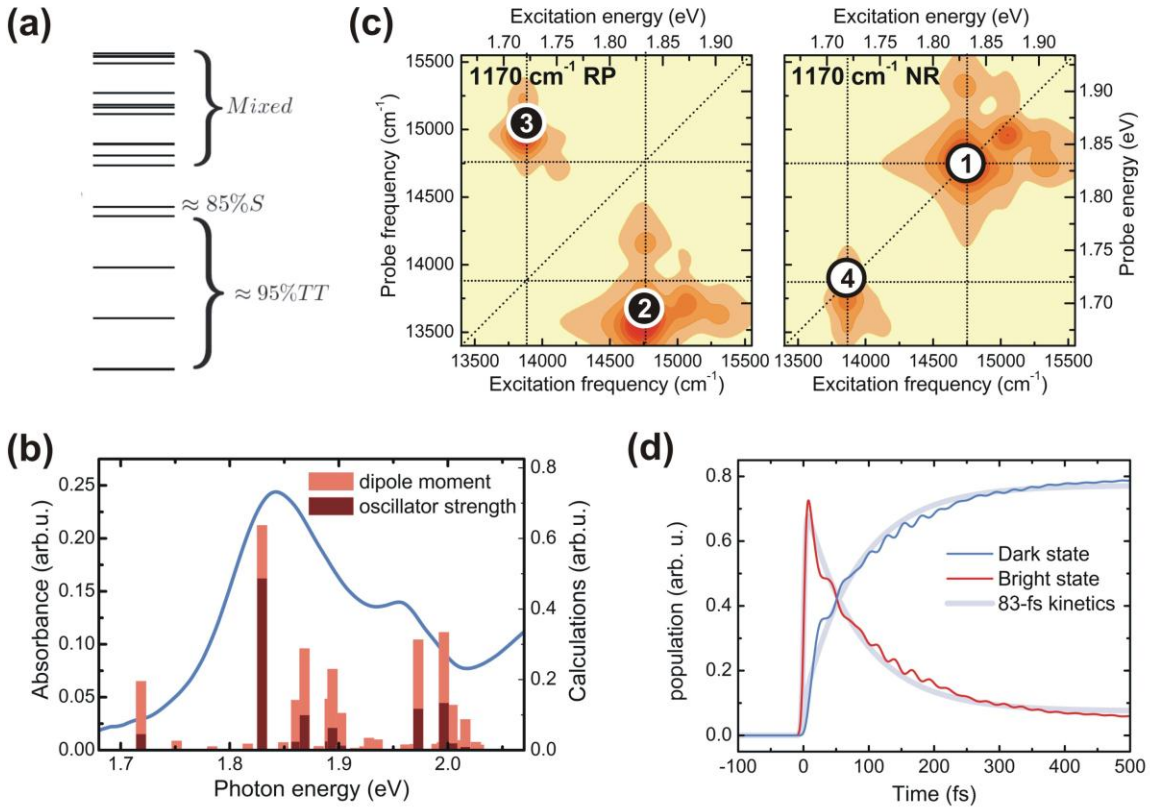

Figure 6. *The results of theoretical calculation based on the vibronic state model. (a) The diagram of eigenstates formed as a result of mixing between the singlet and multiexciton manifold. (b) The calculated dipole moments and oscillator strengths for the eigenstates; the blue curve shows an experimental absorption spectrum for comparison. (c) Calculated rephasing/non-rephasing beating maps for pentacene at 1170 cm^{-1}. The same beating features as in the figure 5a,b are shown with black and white circles. (d) The population kinetics for dark and bright states predicted by the model. The grey curves indicated the 83-fs dynamics deduced from the decay-associated spectra analisys (fig. 3a).*

References:

1. Smith, M.B. & Michl, J. Singlet Fission. *Chemical Reviews* **110**, 6891-6936 (2010).
2. Wilson, M.W.B. *et al.* Ultrafast Dynamics of Exciton Fission in Polycrystalline Pentacene. *Journal of the American Chemical Society* **133**, 11830-11833 (2011).
3. Hanna, M.C. & Nozik, A.J. Solar conversion efficiency of photovoltaic and photoelectrolysis cells with carrier multiplication absorbers. *Journal of Applied Physics* **100**, - (2006).
4. Ehrler, B., Wilson, M.W., Rao, A., Friend, R.H. & Greenham, N. Singlet Exciton Fission-Sensitized Infrared Quantum Dot Solar Cells. *Nano Letters* (2012).
5. Congreve, D.N. *et al.* External Quantum Efficiency Above 100% in a Singlet-Exciton-Fission–Based Organic Photovoltaic Cell. *Science* **340**, 334-337 (2013).
6. Burdett, J.J. & Bardeen, C.J. The Dynamics of Singlet Fission in Crystalline Tetracene and Covalent Analogs. *Accounts Chem. Res.* **46**, 1312-1320 (2013).
7. Dillon, R.J., Piland, G.B. & Bardeen, C.J. Different Rates of Singlet Fission in Monoclinic versus Orthorhombic Crystal Forms of Diphenylhexatriene. *Journal of the American Chemical Society* **135**, 17278-17281 (2013).
8. Mastron, J.N., Roberts, S.T., McAnally, R.E., Thompson, M.E. & Bradforth, S.E. Aqueous colloidal acene nanoparticles: A new platform for studying singlet fission. *Journal of Physical Chemistry B* **117**, 15519-15526 (2013).
9. Lee, J. *et al.* Singlet Exciton Fission in a Hexacene Derivative. *Advanced Materials* **25**, 1445-1448 (2013).
10. Musser, A.J. *et al.* Activated Singlet Exciton Fission in a Semiconducting Polymer. *Journal of the American Chemical Society* **135**, 12747-12754 (2013).
11. Yost, S.R. *et al.* A transferable model for singlet-fission kinetics. *Nat Chem* **6**, 492-497 (2014).
12. Herz, J. *et al.* Acceleration of singlet fission in an aza-derivative of TIPS-pentacene. *Journal of Physical Chemistry Letters* **5**, 2425-2430 (2014).
13. Busby, E. *et al.* Multiphonon Relaxation Slows Singlet Fission in Crystalline Hexacene. *Journal of the American Chemical Society* **136**, 10654-10660 (2014).
14. Beljonne, D., Yamagata, H., Brédas, J.L., Spano, F.C. & Olivier, Y. Charge-Transfer Excitations Steer the Davydov Splitting and Mediate Singlet Exciton Fission in Pentacene. *Physical Review Letters* **110**, 226402 (2013).
15. Johnson, J.C., Nozik, A.J. & Michl, J. The Role of Chromophore Coupling in Singlet Fission. *Accounts Chem. Res.* **46**, 1290-1299 (2013).
16. Zimmerman, P.M., Musgrave, C.B. & Head-Gordon, M. A Correlated Electron View of Singlet Fission. *Accounts Chem. Res.* **46**, 1339-1347 (2013).
17. Wang, L., Olivier, Y., Prezhdo, O.V. & Beljonne, D. Maximizing Singlet Fission by Intermolecular Packing. *The Journal of Physical Chemistry Letters* **5**, 3345-3353 (2014).
18. Berkelbach, T.C., Hybertsen, M.S. & Reichman, D.R. Microscopic theory of singlet exciton fission. III. Crystalline pentacene. *The Journal of Chemical Physics* **141**, - (2014).
19. Zimmerman, P.M., Zhang, Z. & Musgrave, C.B. Singlet fission in pentacene through multi-exciton quantum states. *Nat Chem* **2**, 648-652 (2010).
20. Zeng, T., Ananth, N. & Hoffmann, R. Seeking Small Molecules for Singlet Fission: A Heteroatom Substitution Strategy. *Journal of the American Chemical Society* **136**, 12638-12647 (2014).
21. Coto, P.B., Sharifzadeh, S., Neaton, J.B. & Thoss, M. Low-Lying Electronic Excited States of Pentacene Oligomers: A Comparative Electronic Structure Study in the Context of Singlet Fission. *Journal of Chemical Theory and Computation* **11**, 147-156 (2014).
22. Parker, S.M., Seideman, T., Ratner, M.A. & Shiozaki, T. Model Hamiltonian Analysis of Singlet Fission from First Principles. *The Journal of Physical Chemistry C* **118**, 12700-12705 (2014).
23. Merrifield, R.E., Avakian, P. & Groff, R.P. Fission of singlet excitons into pairs of triplet excitons in tetracene crystals. *Chemical Physics Letters* **3**, 386-388 (1969).

24. Smith, M.B. & Michl, J. Recent Advances in Singlet Fission. *Annual Review of Physical Chemistry* **64**, 361-386 (2013).
25. Chan, W.-L. *et al.* Observing the Multiexciton State in Singlet Fission and Ensuing Ultrafast Multielectron Transfer. *Science* **334**, 1541-1545 (2011).
26. Chan, W.-L., Ligges, M. & Zhu, X.Y. The energy barrier in singlet fission can be overcome through coherent coupling and entropic gain. *Nat Chem* **4**, 840-845 (2012).
27. Alguire, E.C., Subotnik, J.E. & Damrauer, N.H. Exploring Non-Condon Effects in a Covalent Tetracene Dimer: How Important Are Vibrations in Determining the Electronic Coupling for Singlet Fission? *The Journal of Physical Chemistry A* **119**, 299-311 (2015).
28. Renaud, N. & Grozema, F.C. Intermolecular Vibrational Modes Speed Up Singlet Fission in Perylenediimide Crystals. *The Journal of Physical Chemistry Letters* **6**, 360-365 (2014).
29. Musser, A.J. *et al.* Evidence for conical intersection dynamics mediating ultrafast singlet exciton fission. *Nat Phys* **11**, 352-357 (2015).
30. Jonas, D.M. Two-dimensional femtosecond spectroscopy. *Ann.Rev.Phys.Chem.* **54**, 425-463 (2003).
31. Egorova, D. Detection of electronic and vibrational coherences in molecular systems by 2D electronic photon echo spectroscopy. *Chem. Phys.* **347**, 166-176 (2008).
32. Butkus, V., Zigmantas, D., Valkunas, L. & Abramavicius, D. Vibrational vs. electronic coherences in 2D spectrum of molecular systems. *Chemical Physics Letters* **545**, 40-43 (2012).
33. Egorova, D. Self-Analysis of Coherent Oscillations in Time-Resolved Optical Signals. *The Journal of Physical Chemistry A* **118**, 10259-10267 (2014).
34. Brixner, T., Stenger, J., Vaswani, H.M., Blankenship, R.E. & Fleming, G.R. Two-dimensional spectroscopy of electronic couplings in photosynthesis. *Nature* **343**, 625-628 (2005).
35. Ostroumov, E.E., Mulvaney, R.M., Cogdell, R.J. & Scholes, G.D. Broadband 2D Electronic Spectroscopy Reveals a Carotenoid Dark State in Purple Bacteria. *Science* **340**, 52-56 (2013).
36. Halpin, A. *et al.* Two-dimensional spectroscopy of a molecular dimer unveils the effects of vibronic coupling on exciton coherences. *Nat Chem* **6**, 196-201 (2014).
37. Tiwari, V., Peters, W.K. & Jonas, D.M. Electronic resonance with anticorrelated pigment vibrations drives photosynthetic energy transfer outside the adiabatic framework. *Proceedings of the National Academy of Sciences* **110**, 1203-1208 (2013).
38. Lazonder, K., Pshenichnikov, M.S. & Wiersma, D.A. Easy Interpretation of Optical Two-Dimensional Correlation Spectra. *Opt.Lett.* **31**, 3354-3356 (2006).
39. Panitchayangkoon, G. *et al.* Long-lived quantum coherence in photosynthetic complexes at physiological temperature. *Proceedings of the National Academy of Sciences* **107**, 12766-12770 (2010).
40. Bayliss, S.L. *et al.* Geminate and Nongeminate Recombination of Triplet Excitons Formed by Singlet Fission. *Physical Review Letters* **112**, 238701 (2014).
41. Wilson, M.W.B., Rao, A., Ehrler, B. & Friend, R.H. Singlet Exciton Fission in Polycrystalline Pentacene: From Photophysics toward Devices. *Accounts Chem. Res.* **46**, 1330-1338 (2013).
42. Rao, A. *et al.* Exciton fission and charge generation via triplet excitons in pentacene/C60 bilayers. *Journal of the American Chemical Society* (2010).
43. Egorova, D. Oscillations in two-dimensional photon-echo signals of excitonic and vibronic systems: Stick-spectrum analysis and its computational verification. *The Journal of Chemical Physics* **140**, - (2014).
44. De Boeij, W.P., Pshenichnikov, M.S. & Wiersma, D.A. System-bath correlation function probed by conventional and time-gated stimulated photon echo. *Journal of Physical Chemistry* **100**, 11806-11823 (1996).
45. Song, Y., Hellmann, C., Stingelin, N. & Scholes, G.D. The separation of vibrational coherence from ground- and excited-electronic states in P3HT film. *The Journal of Chemical Physics* **142**, 212410 (2015).

46. Schlau-Cohen, G.S. *et al.* Elucidation of the timescales and origins of quantum electronic coherence in LHCII. *Nat Chem* **4**, 389-395 (2012).
47. Egorova, D. & Domcke, W. Coherent vibrational dynamics during ultrafast photoinduced electron-transfer reactions: quantum dynamical simulations within multilevel Redfield theory. *Chemical Physics Letters* **384**, 157-164 (2004).
48. Chan, W.-L., Tritsch, J.R. & Zhu, X.Y. Harvesting Singlet Fission for Solar Energy Conversion: One- versus Two-Electron Transfer from the Quantum Mechanical Superposition. *Journal of the American Chemical Society* **134**, 18295-18302 (2012).
49. Falke, S.M. *et al.* Coherent ultrafast charge transfer in an organic photovoltaic blend. *Science* **344**, 1001-1005 (2014).
50. Romero, E. *et al.* Quantum coherence in photosynthesis for efficient solar-energy conversion. *Nat Phys* **10**, 676-682 (2014).